Remobilization of Deep Basin Brine during Exhumation of the Illizi Basin, Algeria

Kara L. English[1,2], Joseph M. English[1], Jonathan Redfern[2], Cathy Hollis[2], Dermot V. Corcoran[1], Norman Oxtoby[3], Rachida Yahia Cherif[4]

[1]Petroceltic International Plc, 3 Grand Canal Plaza, Grand Canal Street Upper, Dublin 4, Ireland.

[2]School of Earth, Atmospheric and Environmental Sciences, University of Manchester, Williamson Building, Oxford Road, Manchester, M13 9PL, United Kingdom.

[3]Department of Earth Sciences, Royal Holloway, University of London, Egham, Surrey, TW20 0EX, United Kingdom.

[4]Direction Coordination Groupe Associations – Sonatrach, Djenane El-Malik, Hydra, Algiers, Algeria.

Submitted to *Marine and Petroleum Geology*, December 1st, 2015

Revision submitted to *Marine and Petroleum Geology*, June 10th, 2016

Second revision submitted to *Marine and Petroleum Geology*, July 22nd, 2016

Main text word count = 4009

Abstract word count = 163

Number of references = 66

Number of tables = 2

Number of figures = 7

Data Repository = No

Corresponding author = Kara English

Abstract

Understanding the processes that drive fluid flow in sedimentary basins has important implications for models of metallic ore and petroleum migration and accumulation in the subsurface. Potential drive mechanisms include gravity-driven flow, compaction-driven flow, and density-driven convection. In this study, we demonstrate that the brine hosted in Ordovician sandstone in the Illizi Basin in Algeria is genetically linked to Triassic-Liassic evaporites deposited > 400 km to the north in the Berkine Basin. This observation confirms that long distance, lateral, brine migration has occurred within the basin in the past. We assess the hydrogeologic record preserved in aqueous fluid inclusions within the Ordovician sandstone, document a marked increase in formation water salinity during cooling and exhumation, and evaluate the drive mechanisms for late-stage remobilization of deep brines within the basin. It is hypothesized that the release of overpressure during exhumation of the Illizi Basin may have been a critical contributor to updip fluid flux. This model could be applicable to other exhumed basins worldwide.

1. Introduction

Understanding the processes that drive fluid flow in sedimentary basins has important implications for models of metallic ore and petroleum migration and accumulation in the subsurface. A number of different mechanisms have been proposed for driving regional fluid flow in sedimentary basins (e.g. Bethke, 1985; 1989; Bjørlykke, 1993, 2015; Cathles and Adams, 2005; Chi and Xue, 2011; Frazer et al., 2014): (1) topographic or gravity-driven flow, (2) sedimentary or tectonic compaction-driven flow, and (3) thermal- or salinity-driven convection. In this study, we present new compositional analysis of formation water hosted in Ordovician sandstone in the Illizi Basin in Algeria, and demonstrate that this brine is genetically linked to Triassic-Liassic evaporites deposited in the Berkine Basin to the north (Fig. 1). Building on previous thermal history modelling of the area (English et al., 2016b, 2016c), we assess the hydrogeologic record preserved in aqueous fluid inclusions in order to constrain the timing of brine migration into the Ordovician sandstone in the Illizi Basin, and we evaluate overpressure dissipation during exhumation as a potential drive mechanism for late-stage remobilization of deep brines. This model could be applicable to other exhumed basins worldwide and has implications for the timing and direction of major fluxes of deep basin brines in the geological record.

2. Geological history of the Illizi Basin

Following the Late Neoproterozoic Pan-African orogeny, the northern margin of Gondwana was characterized by a vast clastic-dominated Paleozoic sedimentary basin on the edge of the ProtoTethys (Beuf et al., 1971; Stampfli and Borel, 2002; Guiraud et al., 2005). During the collision of Gondwana with Laurasia, the Late Carboniferous-Early Permian Hercynian (Variscan) Orogeny caused extensive uplift and erosion along north–south trending arches in northwest Africa (Aliev et al., 1971; Burollet et al., 1978; Boote et al., 1998; Acheche et al., 2001). Erosion removed the post-Cambro-Ordovician sequence on some of these uplifted arches, but the majority of the Paleozoic sequence was preserved in the Illizi Basin (Galeazzi et al., 2010; English et al., 2016c; Fig. 2). Renewed deposition of the Mesozoic–early Cenozoic “Tethys Supersequence” (Boote et al., 1998) in North Africa followed the opening of the Tethyan seaway, and a Triassic salt basin developed to the north of the Illizi Basin in the Berkine and Oued Mya basins (Turner and Sherif, 2007; Galeazzi et al., 2010). Mesozoic-Cenozoic deposition in the region was punctuated by Early-Mid Aptian

transpression and strike-slip deformation during the Austrian event (Boudjema, 1987; Galeazzi et al., 2010), and by Mid-Late Eocene inversion that caused growth of the Atlas range to the north (Echikh, 1998). Intraplate uplift and magmatism also initiated in North Africa during the Mid-Late Eocene (Wilson and Guiraud, 1992; Wilson et al., 1998; Liégeois et al., 2005) leading to the development of numerous topographic swells and large-scale exhumation of flanking sedimentary basins such as the Illizi and Tim Mersoï basins (English et al., 2016b).

The new data in this study comes from an Ordovician sandstone reservoir in a gas-condensate field located in the southern Illizi Basin (Fig. 1). Previous studies have constrained the burial and thermal history of the study area through integration of regional stratigraphy, sonic compaction analysis, biostratigraphy, thermal maturity, fluid inclusion microthermometry, and apatite fission-track data (English et al., 2016b; 2016c). These studies confirmed that the preserved Paleozoic sequence in the Illizi Basin was subjected to elevated temperatures in the past, initially because of additional burial prior to Hercynian exhumation, and again during reburial in the Mesozoic and early Cenozoic (Fig. 2). The available data indicate that maximum burial most likely occurred during the early Eocene, prior to uplift of the Hoggar massif and northward tilting of the Illizi Basin (English et al., 2016b). Based on 1-dimensional (1D) modelling, maximum burial depths for the Top Ordovician are estimated at 2.95 km in the northern part of the field (Well A) and 3.37 km in the southern part of the field (Well G), and the corresponding estimates of maximum paleotemperature are 140°C and 156°C respectively (English et al., 2016c). The magnitudes of subsequent Cenozoic exhumation are estimated at 1.0 km and 1.4 km for the northern (Well A) and southern (Well G) areas respectively. Based on the modelling of English et al. (2016c), hydrocarbon generation from the lower Silurian source rocks is interpreted to have started during the Carboniferous, ceased temporarily during Hercynian exhumation, and subsequently resumed in the Mesozoic following renewed subsidence (Fig. 2). Trap formation in the study area occurred during the Eocene-Miocene regional tilting of the Illizi Basin, after the primary hydrocarbon generation events, and alternative charging mechanisms have been proposed including (1) long-distance migration from an active source area; (2) remigration of existing hydrocarbons within the basin; (3) phase separation and gas expansion within exhumed preexisting oil and gas accumulations; and/or (4) late-stage exhumation charge during the depressuring of the overlying source rocks (English et al. 2016c).

3. Methods

Four samples of formation water were collected at surface during flow testing of the Ordovician sandstone reservoir at two different wells (Well D and Well H) in the study area (Fig. 1). The Ordovician sandstone occurs at a depth of ~2 km in the area present-day. The water samples were sent for compositional analysis at Expro's laboratory in Chandlers Ford, UK. All cations (except ammonium and tetramethylammonium) were determined by inductively coupled plasma (ICP), while ammonium and tetramethylammonium were determined by colorimetry and ion chromatography respectively. Most of the anions were determined by ion chromatography, while the acid anions and bicarbonate concentrations were determined by ion exclusion chromatography, and chloride was determined by potentiometric titration.

Fluid inclusion analysis was carried out on 39 Ordovician Unit IV sandstone samples from across seven wells (Wells A through G) in a gas-condensate field in the study area (Fig. 1). Aqueous and petroleum inclusions were observed as primary inclusions within quartz overgrowths, along quartz grain boundaries and in parageneticallly-late barite cement, and as secondary inclusions in healed microfractures. The homogenization temperature (T_h) of each inclusion was determined optically by incrementally heating the sample until a vapour bubble dissipated into the inclusion (Goldstein and Reynolds, 1994; Walderhaug, 1994). The final melting temperature was measured by initially freezing the samples and recording the temperature of the final disappearance of solid during subsequent heating. The salinity of the aqueous inclusions can then be estimated from the ice-melting temperatures (Oakes et al., 1990; Bodnar, 1993).

4. Results

The present-day formation water of the Ordovician sandstone in the study area is a sodium- and calcium-rich (Na-Ca-Cl) brine characterized by little to no sulfate and bicarbonate (Table 1). The total dissolved solids (TDS) content of the samples is uniformly in the 158-161 g/l range. The chloride contents in all four samples are consistently in the 95-98 g/l range and constitute > 99% of the anionic species. The sodium content varies between 33-37 g/l, and constitutes 50-60% of the cationic species. Calcium is the second major cation

(~30%), and magnesium and potassium are present only in relatively minor concentrations (< 5% each). All four samples have low Cl/Br and Na/Br mass ratios (~113 and ~41 respectively).

The fluid inclusion dataset is dominated by two distinct groups of aqueous inclusions (Table 2; Fig. 3): (1) low-to-high temperature, low-salinity (4-8 wt.%) inclusions, and (2) low temperature, high-salinity (18-25 wt.%) inclusions, with an additional smaller number of inclusions with intermediate temperature and salinity between the two end-member groups. All salinities quoted herein are NaCl equivalent. The salinity of the first group of inclusions predominantly ranges between 4-8 wt.%, and homogenization temperatures extend from 95°C up to modal values of 135-155°C. This family of aqueous inclusions co-occurs with single-phase oil inclusions at close to full gas saturation, determined by the similarity of T_h in both aqueous and oil inclusions (Munz, 2001). The second distinct group of aqueous inclusions is characterized by significantly higher salinities of 18-25 wt.% and by cooler modal homogenization temperatures of 90-120°C (Table 2; Fig. 3). Low temperature, high-salinity (~18 wt.%) inclusions are also hosted in barite cement (Fig. 3A) and are associated with phase-separated oil and associated gas inclusions. Further details on the petroleum inclusions from this dataset can be found in English et al. (2016c).

It is noteworthy that the high-salinity inclusions are not observed to coincide with maximum burial temperatures indicating that these inclusions record either early (pre-maximum burial) or late (post-maximum burial) fluid compositions. Petrographic evidence indicating that the high-salinity aqueous inclusions post-date the low-salinity aqueous inclusions is summarized in Figure 4.

1. Primary aqueous inclusions trapped in barite cement in Well A yield homogenization temperatures (98–115°C) and salinities (18–19 wt.%) that are relatively similar to the present-day reservoir temperature (~95°C) and formation water salinity (~14.5 wt.%). Barite occurs as late-stage pore-filling or replacive cement and generally encloses and post-dates all the quartz cement phases (Fig. 4A); the lower salinity primary fluid inclusions in Well A are exclusively hosted in these earlier quartz cements.
2. In Well B, all of the primary aqueous inclusions are hosted in quartz overgrowths and are from the lower salinity group. However, secondary aqueous oil-associated inclusions in a healed microfracture are observed to

cross-cut a quartz overgrowth and detrital grain (Fig. 4B) and therefore post-date the initial quartz overgrowths. These secondary inclusions have higher salinity (14–15 wt.%) and lower homogenization temperatures (108–130°C) than the primary quartz inclusions, which again suggests that the higher salinity inclusions are younger.

3. The clearest evidence for the relative timing of the two distinct fluid inclusion groups comes from Well D (Fig. 4C). Higher salinity (17.2 wt.%) secondary aqueous inclusions, with homogenization temperatures of 122–124°C, are observed within a healed microfracture that cuts across a quartz cement overgrowth (and detrital quartz grain) that contains primary inclusions of lower salinity (7–8 wt.%) formed at higher temperatures (145–170°C).

5. Origin of formation water in Ordovician sandstone

The high salinity of brines is often associated with halite intervals within sedimentary basins. The brines may form either initially through the progressive evaporation of seawater or through dissolution of marine evaporites such as halite (Hanor, 1994). Na-Cl-Br systematics of basinal brines can be used to shed light on their genesis (Rittenhouse, 1967; Carpenter, 1978; Walter et al., 1990; Kesler et al., 1995). Fluid Cl/Br and Na/Br ratios remain constant during progressive evaporation of seawater to the point of halite precipitation, but these ratios start to progressively decrease during subsequent halite, Mg-salt and K-salt precipitation as Br is preferentially retained in the fluid phase (Fig. 5). Conversely, the dissolution of halite will act to increase these ratios because halite is relatively deficient in Br. These ratios are not impacted by subsequent dilution with meteoric water (Kesler et al., 1995).

The formation water in this study is characterized by low Cl/Br (~113) and Na/Br (~41) mass ratios relative to seawater (292 and 162 respectively; Carpenter, 1978), and this is consistent with genesis from the progressive evaporation of seawater beyond the point of halite precipitation (Fig. 5). The Paleozoic sequence of the Illizi Basin is dominated by clastic sediments deposited within fluvial, deltaic and marine conditions, and evaporitic sequences were not deposited in the region until the Triassic–Lower Jurassic (Turner and Sherif, 2007). This evaporitic basin was situated across the Berkine and Oued Mya basins, and did not extend as far south as the study area in the southern Illizi Basin (Fig. 1). A comparison with

published water analyses from the Triassic reservoir sandstones of the El Borma Field in the Berkine-Ghadames Basin (Morad et al., 1994) confirms that the Ordovician formation waters in the study area have a similar Na-Cl-Br signature to the Triassic brines (Fig. 5). Hence, it is probable that the highly saline formation waters present in the Ordovician sandstones in the Illizi Basin are originally derived from the younger Triassic section in the Berkine Basin, deposited over 400 km to the north (Fig. 1). Calcium-rich brines with salinities in excess of 25 wt.% have also been reported from Ordovician rocks in the Hassi Messaoud area by Chiarelli (1973), where the Triassic sequence, including halite, is situated directly on top of Cambro-Ordovician strata (Fig. 6; Bacheller and Peterson, 1991).

Abnormally high pressures originate in undercompacted shales sealed by the impermeable salt in the present-day Hassi Messaoud region, and the Oued Mya and Berkine basins (Chiarelli, 1978; Yahi et al., 2001). Mesozoic sediments were deposited directly on Cambro-Ordovician rocks in parts of the basin characterized by deep Hercynian incision (Fig. 1; Zeroug et al., 2007; Galeazzi et al., 2010). High-salinity brines may, therefore, have originally infiltrated into the Cambro-Ordovician sequence at these locations (north of the study area; Fig. 6) by density-driven brine reflux (e.g. Bein and Dutton, 1993; Ceriani et al., 2002) during or after the deposition of the evaporitic sequence or by relative overpressuring in the Mesozoic subsalt formations adjacent to Ordovician subcrops (Chiarelli, 1978).

6. Temporal evolution of Ordovician formation water

Fluid inclusions are commonly utilized in thermal history, diagenetic and petrographic studies to elucidate the temperature and salinity record of trapped liquid and/or vapour inclusions (Roedder, 1984; Walderhaug, 1994; Goldstein, 2001; Blanchet et al., 2003). It has been demonstrated the fluid inclusion dataset is dominated by two distinct groups of aqueous inclusions (Figs. 3 and 4). The low salinity of the first group of inclusions (4-8 wt.%), and associated homogenization temperatures, record cementation from the onset of quartz diagenesis at 95°C up to likely maximum burial temperatures of 135-155°C (Figs. 2 and 4; English et al., 2016c; English et al., in review B). This family of aqueous inclusions co-occurs with single-phase oil inclusions indicating that oil generation also took place in the basin during this time. In contrast, the higher salinities (18-25 wt.%) and cooler modal homogenization temperatures (90-120°C) of the second distinct group of secondary aqueous inclusions (Table 2; Fig. 3) occur within microfractures that crosscut quartz overgrowths

containing low-salinity inclusions (Fig. 4). Consequently, the high-salinity (and lower temperature) inclusions are interpreted to post-date the low-salinity (and higher temperature) inclusions (Figs. 2 and 4). A subset of inclusions with intermediate salinities (10-18 wt.%) and homogenization temperatures (Table 2; Fig. 3) may record the transition from one formation water type to the other.

The homogenization temperatures of the high-salinity inclusions are most similar to present-day temperatures within the Ordovician sandstone in the study area (95-100°C), although the present-day formation water salinity is a little lower, at ~14.5 wt.% (Table 1; Figs. 3 and 4). Additionally, the low temperature, high-salinity aqueous inclusions hosted in paragenetically-late barite have salinities of ~18 wt.%, and hence manifest the closest characteristics to the present-day formation water (Fig. 4A). In conclusion, the fluid inclusion dataset from the Ordovician sandstones of the Illizi Basin are interpreted to record a significant increase in formation water salinity after, or during, Cenozoic exhumation and cooling (Fig. 2). Phase-separated oil and associated gas are observed in petroleum inclusions in the late-stage barite cement (English et al., 2016c) indicating both gas and oil were present in the pore system during exhumation and cooling, unlike the higher temperature petroleum inclusions that are characterized by single-phase oils.

Comparing the connate (original) and present-day salinities in a given stratigraphic unit can provide important insights for bulk transport fluid flow models. The Lower Paleozoic section of the Illizi Basin was deposited in fluvial, deltaic and normal marine environments, and it can be surmised that the original connate water in the Ordovician sandstone during time of deposition was unlikely to be significantly in excess of normal seawater salinity (~35 g/l). This is in sharp contrast to the present-day formation water salinity of ~160 g/l (Table 1) indicating that large-scale vertical or lateral transport of brine into the study area occurred at some point during the history of the basin.

Formation water salinity-depth trends have been described in many different sedimentary basins around the world (e.g. Dickey, 1966; 1969; Hanor, 1979; 1994; Gran et al., 1992). Figure 7 illustrates two such trends from (1) Jurassic to Cretaceous strata in southern Arkansas and northern Louisiana (Dickey, 1969), and (2) the northern North Sea (Gran et al., 1992). There is a pronounced increase in salinity with depth in the Gulf Coast example, and salinities approach values of 350,000 ppm at a depth of ~3 km (Fig. 7). The high-salinity brines in this region are interpreted to be derived in part from an underlying evaporitic unit (Moldovanyi and Walter, 1992; Hanor, 1994). In contrast, there is no

significant increase in salinity with depth in the northern North Sea example (Fig. 7), where no underlying evaporites are known to occur (Gran et al., 1992; Bjørlykke and Gran, 1994).

In comparison, the high temperature, low-salinity fluid inclusions from the Illizi Basin study area lie along the northern North Sea trend (Fig. 7), which suggests that no significant mixing with evaporitic brines occurred during burial or at maximum burial conditions. As per the northern North Sea example, no evaporites were present in the study area because the depositional edge of the Triassic salt basin was situated much further north (Figs. 1 and 6). In contrast, the low temperature, high-salinity fluid inclusion group from the study area plots on the southern Arkansas-northern Louisiana trend (Fig. 7), consistent with the proposed derivation from an evaporitic source, as demonstrated for the present-day formation water (Fig. 5). This dramatic change in the salinity-depth relationship recorded by the fluid inclusion dataset confirms that a significant lateral transport of brine occurred within the basin, and the thermal record of the fluid inclusions confirms that this fluid flow event occurred during or after exhumation (Figs. 2, 4 and 7).

7. Updip migration of deep brine during exhumation

Formation water in the subsurface may be characterized by static or dynamic conditions. Hydrodynamic flow in sedimentary basins is driven by spatial variations in water potential (Hubbert, 1953; England et al., 1987), and can occur as a result of (e.g. Bethke, 1989; Bjørlykke, 1993, 2015): (1) gravity-driven flow of meteoric water downwards into the basin caused by an elevated water table on the uplifted basin margins; (2) sedimentary or tectonic compaction-driven flow upward and outward from the basin center caused by fluid overpressure generated during burial by compaction, clay mineral diagenesis and petroleum generation; (3) density-driven flow caused by thermal or salinity gradients which may initiate convection. Potentiometric maps from the Illizi and Berkine basins in Algeria indicate the presence of both an active gravity-flow hydrodynamic regime on the southern flank of the Illizi Basin, and an overpressured system beneath the Triassic salts of the Berkine Basin (Figs. 1 and 6; Chiarelli, 1978).

Although present-day potentiometric maps for the Cambro-Ordovician in the Illizi Basin suggest northward hydrodynamic flow of meteoric water from elevated outcrops in the south (Chiarelli, 1978), the fluid inclusion data presented here indicate that exhumation of the Illizi Basin was associated with a major flux of highly saline brines that most likely

originated from the salt-rich section to the north of the study area (Fig. 6). Triassic deposits directly overlie Cambro-Ordovician strata along major Hercynian structures (Fig. 1), and the high-salinity brines may have originally infiltrated the Cambro-Ordovician sequence at these locations via density-driven brine reflux during or after the deposition of the Triassic evaporitic sequence. Lateral flow within the Cambro-Ordovician sequence is interpreted to have been focused between the underlying crystalline basement and the overlying compacted Lower Silurian shales, and may also have been facilitated by natural fracture systems within the sandstone-dominated sequence. Compaction-driven lateral flow is ruled out on the basis that the Illizi Basin was undergoing exhumation during precipitation of the cements containing the lower temperature/higher salinity fluids (Fig. 2), and deposition had largely ceased in the Berkine Basin to the north. Rayleigh convection is ruled out on the basis that it requires thick sequences (100-300 m) of homogeneous and porous sandstones with no interbedded thin shales or cemented intervals (Bjørlykke et al., 1988). Additionally, the apparent updip migration of higher salinity brine, displacing less dense and lower salinity formation water, indicates that density contrast was not a driving factor for the fluid flow.

Instead, we propose that breaching of a closed, relatively overpressured system during basin exhumation is an alternative mechanism for regional updip flow of formation water. New discharge sites were created along the newly exposed southern margin of the basin during the Cenozoic (Fig. 6) and opening of the basin margin to normal hydrostatic conditions during exhumation could have generated the required regional lateral gradient in fluid potential (i.e. relatively overpressured conditions to the north and normal hydrostatic conditions to the south). Alternatively, if the original overpressure in the basin was laterally discontinuous and compartmentalized by faulting, it is possible that some of these faults may have become critically-stressed (Barton et al., 1995) during the removal of overburden during exhumation (e.g. Corcoran and Doré, 2002; English et al., in review A). This would lead to the progressive release of overpressured fluid through frictional sliding along optimally-oriented pre-existing faults (Sibson, 2000; Finkbeiner et al., 2001) during exhumation until the system regains equilibrium. Recent geomechanical analysis in the study area has confirmed that the primary N-S and NW-SE fault systems in this part of the Illizi Basin are likely to be critically stressed under the present-day *in situ* stress conditions (English et al., in review A).

The fluid flow resulting from pressure release may be restricted to a geologically short time period, depending on distance and effective permeability, because equilibration of

unsteady state pressure distributions is one of the quickest mixing processes for subsurface fluids (e.g. Smalley and Muggeridge, 2010). The volume of fluid flux may also be somewhat limited because of the low compressibility of water (Bjørlykke, 1993, 2015). However, if overpressure release results in increased effective stress in deeper, less exhumed parts of the basin, additional compaction and pore-volume loss may supplement the updip fluid flow. Additionally, volumetric expansion of *in situ* gaseous hydrocarbons during basin exhumation (e.g. Doré and Jensen, 1996; Doré et al., 2002; English et al., 2016c), exhumation charge from petroleum source rocks (English et al., 2016a), and methane exsolution from formation water may also serve to displace significant additional volumes of formation water updip if these incremental hydrocarbon volumes are trapped within the basin.

Following the removal of the lateral gradient in fluid potential due to the bleed-off of excess pressure, subsequent fluid-flow reversal by gravity-driven flow of meteoric water from the basin margins may have become more well established (Fig. 6). This could account for the decreased salinity in the present-day formation water (~14.5 wt.%) compared to the higher salinity of the migrated basinal brines (low-temperature aqueous inclusions >18 wt.%; Figs. 3A and 4). Additionally, the mixing of barium-rich brines with sulfate-rich meteoric waters may also account for the precipitation of late-stage barite cement found in permeable beds (>50 md) within the Upper Ordovician (Fig. 4A; English et al., 2016c; in review B). Chiarelli (1973, 1978) has also noted the deep invasion of relatively freshwater in shallower stratigraphic zones in the Illizi Basin with salinities < 0.5 wt.% being present in Devonian sandstones up to 200 km north of their southern outcrops.

8. Conclusions

Existing drive mechanisms for fluid flow in sedimentary basins include gravity-driven flow, compaction-driven flow, and density-driven convection. Interrogation of fluid inclusion and present-day water chemistry data from Ordovician sandstones confirms that long distance, lateral, brine migration and mixing have occurred within the Illizi Basin, Algeria. The Na-Cl-Br characteristics of the Ordovician sandstone formation water in the study area is consistent with derivation from the Triassic-Liassic halite-bearing sequence deposited in the Berkine Basin, which is located > 400 km to the north. The hydrogeologic record preserved by fluid inclusions within the Ordovician sandstone suggests that an early stage, low-salinity water was displaced by a higher salinity fluid during, and subsequent to, exhumation from

maximum burial depth and temperature. It is proposed that the release of fluid overpressure during exhumation of the Illizi Basin may have been a critical contributor to updip fluid flux. Fluid flux during basin exhumation has not been considered widely in the literature, and this model may have implications for the timing and direction of major fluxes of deep basin brines and associated fluids in the geological record.

Acknowledgements

We thank Petroceltic, Sonatrach and Enel, for sponsoring this study and granting permission for publication. We would also like to acknowledge Mark Andrew for his insight on water chemistry, and the associate editor Hanneke Verweij and two anonymous reviewers for their feedback which helped improve the quality of this manuscript.

References

Acheche, M.H., M'Rabet, A., Ghariani, H., Ouahchi, A., and Montgomery, S.L., 2001, Ghadames basin, southern Tunisia: A reappraisal of Triassic reservoirs and future prospectivity: American Association of Petroleum Geologists Bulletin, v. 85, p. 765-780, doi: 10.1306/8626C9F1-173B-11D7-8645000102C1865D.

Aliev, M., Aït Laoussine, N., Avrov, V., Aleksine, G., Barouline, G., Lakovlev, B., Korj, M., Kouvykine, J., Makarov, V., Mazanov, V., Medvedev, E., Mkrtchiane, O., Moustafinov, R., Oriev, L., Oroudjeva, D., Oulmi, M., and Saïd, A., 1971, Geological structures and estimation of oil and gas in the Sahara in Algeria: Spain, Altamira-Rotopress, S.A., 265 p.

Bacheller, W.D., and Peterson, R.M., 1991, Hassi Messaoud Field – Algeria, Trias Basin, Eastern Sahara Desert, *in* Foster, N.H., and Beaumont, E.A., eds., Structural Traps V, American Association of Petroleum Geologists Treatise of Petroleum Geology, Atlas of Oil and Gas Fields, p. 211–225.

Barton, C.A., Zoback, M.D., and Moos, D., 1995, Fluid flow along potentially active faults in crystalline rock: Geology, v. 23, p. 683-686, doi: 10.1130/0091-7613(1995)023<0683:FFAPAF>2.3.CO;2.

Bein, A., and Dutton, A.R., 1993, Origin, distribution, and movement of brine in the Permian Basin (U.S.A.): A model for displacement of connate brine: Geological Society of America Bulletin, v. 105, p. 695-707, doi: 10.1130/0016-7606(1993)105<0695:ODAMOB>2.3.CO;2.

Bethke, C.M., 1985, A numerical model of compaction-driven groundwater flow and heat transfer and its application to the paleohydrology of intracratonic sedimentary basins: Journal of Geophysical Research, v. 90, p. 6817-6828, doi: 10.1029/JB090iB08p06817.

Bethke, C.M., 1989, Modeling subsurface flow in sedimentary basins: Geologische Rundschau, v. 78, p. 129-154, doi: 10.1007/BF01988357.

Beuf, S., Biju-Duval, B., Charpal O. de, Rognon P., Gariel O., and Bennacef, A., 1971, Les grès du Paléozoïque inférieur au Sahara: Publications de l'Institut Français du Pétrole, Coll. Science et Technique du Pétrole 18, Paris, 464 p.

Bjørlykke, K., 1993, Fluid flow in sedimentary basins: Sedimentary Geology, v. 86, p. 137-158, doi: 10.1016/0037-0738(93)90137-T.

Bjørlykke, K., 2015, Chapter 10: Subsurface water and fluid flow in sedimentary basins, *in* Bjørlykke, K., ed., Petroleum Geoscience: From Sedimentary Environments to Rock Physics: Springer-Verlag, p. 279-300, doi: 10.1007/978-3-642-02332-3_10.

Bjørlykke, K., and Gran, K., 1994, Salinity variations in North Sea formation waters: implications for large-scale fluid movements: Marine and Petroleum Geology, v. 11, p. 5-9, doi: 10.1016/0264-8172(94)90003-5.

Bjørlykke, K., Mo, A., and Palm, E., 1988, Modelling of thermal convection in sedimentary basins and its relevance to diagenetic reactions: Marine and Petroleum Geology, v. 5, p. 338-351, doi: 10.1016/0264-8172(88)90027-X.

Blanchet, A., Pagel, M., Walgenwitz, F., and Lopez, A., 2003, Microspectrofluorometric and microthermometric evidence for variability in hydrocarbon fluid inclusions in quartz overgrowths: implications for inclusion trapping in the Alwyn North field, North Sea: Organic Geochemistry, v. 34, p. 1477-1490, doi: 10.1016/j.orggeochem.2003.08.003.

Bodnar, R.J., 1993, Revised equation and table for determining the freezing point depression of H_2O-NaCl solutions: Geochimica et Cosmochimica Acta, v. 57, p. 683-684, doi: 10.1016/0016-7037(93)90378-A.

Boote, D.R.D., Clark-Lowes, D.D., and Traut, M.W., 1998, Palaeozoic petroleum systems of North Africa, *in* MacGregor, D.S., Moody, R.T.J., and Clark-Lowes, D.D., eds., Petroleum geology of North Africa: Geological Society, London, Special Publication 132, p. 7-68, doi: 10.1144/GSL.SP.1998.132.01.02.

Boudjema, A., 1987, Evolution structural du basin petrolier Triasique du Sahara Nord Oriental (Algérie): Ph.D. thesis, Université de Paris-Sud, Centre d'Orsay, 290 p.

Burollet P., Mugniot, J., and Sweeney, P., 1978, The geology of the Pelagian block: the margins and basins off southern Tunisia and Tripolitania, *in* Nairn, A., Kanes W., and Stehli F., eds., The Ocean Basins and Margins: Springer, p. 331-359, doi: 10.1007/978-1-4684-3039-4_6.

Carpenter, A.B., 1978, Origin and chemical evolution of brines in sedimentary basins: Society of Petroleum Engineers, SPE-7504-MS, doi: 10.2118/7504-MS.

Cathles, L.M., and Adams, J.J., 2005, Fluid flow and petroleum and mineral resources in the upper (<20 km) continental crust, *in* Hedenquist, J.W., Thompson, J.F.H., Goldfarb, R.J., and

Richards, J.P., eds., Economic Geology 100th Anniversary Volume: Society of Economic Geologists, p. 77-110.

Ceriani, A., Di Giulio, A., Goldstein, R.H., and Rossi, C., 2002, Diagenesis associated with cooling during burial: An example from Lower Cretaceous reservoir sandstones (Sirt Basin, Libya): American Association of Petroleum Geologists Bulletin, v. 86, p. 1573-1591, doi: 10.1306/61EEDD0A-173E-11D7-8645000102C1865D.

Chi, G., and Xue, C., 2011, An overview of hydrodynamic studies of mineralization: Geoscience Frontiers, v. 2, p. 423-438, doi: 10.1016/j.gsf.2011.05.001.

Chiarelli, A., 1973, Etude des nappes aquifers profondes: Contribution de l'hydrogéologie à la connaissance d'un bassin sédimentaire et à l'exploration pétrolière: Ph.D. thesis, Université de Bordeaux, France, 197 p.

Chiarelli, A., 1978, Hydrodynamic framework of eastern Algerian Sahara – Influence on hydrocarbon occurrence: American Association of Petroleum Geologists Bulletin, v. 62, p. 667-685.

Corcoran, D.V., and Doré, A.G., 2002, Depressurization of hydrocarbon-bearing reservoirs in exhumed basin settings: evidence from Atlantic margin and borderland basins, *in* Doré, A.G., Cartwright, J.A., Stoker, M.S., Turner, J.P., and White, N., eds., Exhumation of the North Atlantic Margin: Timing, Mechanisms and Implications for Petroleum Exploration: Geological Society, London, Special Publication 196, p. 457-483, doi: 10.1144/GSL.SP.2002.196.01.25.

Dickey, P.A., 1966, Patterns of chemical composition in deep subsurface waters: American Association of Petroleum Geologists Bulletin, v. 50, p. 2472-2478.

Dickey, P.A., 1969, Increasing concentration of subsurface brines with depth: Chemical Geology, v. 4, p. 361-370, doi: 10.1016/0009-2541(69)90055-2.

Doré, A.G., and Jensen, L.N., 1996, The impact of late Cenozoic uplift and erosion on hydrocarbon exploration: offshore Norway and some other uplifted basins: Global and Planetary Change, v. 12, p. 415-436, doi: 10.1016/0921-8181(95)00031-3.

Doré, A.G., Corcoran, D.V., and Scotchman, I.C., 2002, Prediction of the hydrocarbon system in exhumed basins, and application to the NW European margin, *in* Doré, A.G., Cartwright, J.A., Stoker, M.S., Turner, J.P., and White, N., eds., Exhumation of the North

Atlantic Margin: Timing, Mechanisms and Implications for Petroleum Exploration: Geological Society, London, Special Publication 196, p. 401-429, doi: 10.1144/GSL.SP.2002.196.01.21.

Echikh, K., 1998, Geology and hydrocarbon occurrences in the Ghadames Basin, Algeria, Tunisia, Libya, *in* MacGregor, D.S., Moody, R.T.J., and Clark-Lowes, D.D., eds., Petroleum geology of North Africa: Geological Society, London, Special Publication 132, p. 109-129, doi: 10.1144/GSL.SP.1998.132.01.06.

Egeberg, P.K., and Aagaard, P., 1989, Origin and evolution of formation waters from oil fields on the Norwegian shelf: Applied Geochemistry, v. 4, p. 131-142, doi: 10.1016/0883-2927(89)90044-9.

England, W.A., MacKenzie, A.S., Mann, D.M., and Quigley, T.M., 1987, The movement and entrapment of petroleum fluids in the subsurface: Journal of the Geological Society, v. 144, p. 327-347, doi: 10.1144/gsjgs.144.2.0327.

English, J.M., English, K.L., Corcoran, D.V., and Toussaint, F., 2016a, Exhumation charge – the last gasp of a petroleum source rock and implications for unconventional gas: American Association of Petroleum Geologists Bulletin, v. 100, p. 1-16, doi: 10.1306/07271514224.

English, K.L., Redfern, J., Bertotti, G., English, J.M., and Yahia Cherif, R., 2016b, Intraplate uplift: New constraints on the Hoggar dome from the Illizi basin (Algeria): Basin Research, doi: 10.1111/bre.12182.

English, K.L., Redfern, J., Corcoran, D.V., English, J.M., and Yahia Cherif, R., 2016c, Constraining burial history and petroleum charge in exhumed basins: new insights from the Illizi Basin: American Association of Petroleum Geologists Bulletin, v. 100, p. 623-655, doi: 10.1306/12171515067.

English, J.M., Finkbeiner, T., English, K.L., and Yahia Cherif, R., in review A, State of stress in exhumed basins and implications for fluid flow – Insights from the Illizi Basin, Algeria, *in* Healy, D., Hillis, R.R., Turner, J.P., and Welch, M., eds., Geomechanics and Geology: Geological Society, London, Special Publication.

English, K.L., English, J.M., Bonnell, L., Lander, R.H., Hollis, C., Redfern, J., Guirdham, C., Garnham, J., and Yahia Cherif, R., in review B, Controls on reservoir quality in exhumed basins - an example from the Ordovician sandstones, Illizi basin, Algeria: Marine and Petroleum Geology.

Finkbeiner, T., Zoback, M., Flemings, P., and Stump, B., 2001, Stress, pore pressure, and dynamically constrained hydrocarbon columns in the South Eugene Island 330 field, northern Gulf of Mexico: American Association of Petroleum Geologists Bulletin, v. 85, p. 1007-1031.

Frazer, M., Whitaker, F., and Hollis, C., 2014, Fluid expulsion from overpressed basins: Implications for Pb-Zn mineralisation and dolomitisation of the East Midlands platform northern England: Marine and Petroleum Geology, v. 55, p.68-86, doi: 10.1016/j.marpetgeo.2014.01.004.

Galeazzi, S., Point, O., Haddadi, N., Mather, J., and Druesne, D., 2010, Regional geology and petroleum systems of the Illizi–Berkine area of the Algerian Saharan Platform: An overview: Marine and Petroleum Geology, v. 27, p. 143-178, doi: 10.1016/j.marpetgeo.2008.10.002.

Goldstein, R.H., 2001, Fluid inclusions in sedimentary and diagenetic systems: Lithos, v. 55, p. 159-193, doi: 10.1016/S0024-4937(00)00044-X.

Goldstein, R.H., and Reynolds, T.J., 1994, Systematics of fluid inclusions in diagenetic minerals: Society for Sedimentary Geology Short Course 31, 199 p.

Gran, K., Bjørlykke, K., and Aagaard, P., 1992, Fluid salinity and dynamics in the North Sea and Haltenbanken basins derived from well log data, *in* Hurst, A., Griffiths, C.M., and Worthington, P.F., eds., Geological Applications of Wireline Logs II: Geological Society, London, Special Publication 65, p. 327-338, doi: 10.1144/GSL.SP.1992.065.01.25.

Guiraud, R., Bosworth, W., Thierry, J., and Delplanque, A., 2005, Phanerozoic geological evolution of northern and central Africa: An overview: Journal of African Earth Sciences, v. 43, p. 83–143, doi: 10.1016/j.jafrearsci.2005.07.017.

Hanor, J.S., 1979, The sedimentary genesis of hydrothermal fluids, *in* Barnes, H.L., ed., Geochemistry of hydrothermal ore deposits: John Wiley and Sons, New York, p. 137-172.

Hanor, J.S., 1994, Origin of saline fluids in sedimentary basins, *in* Parnell, J., ed., Geofluids: origin, migration and evolution of fluids in sedimentary basins: Geological Society, London, Special Publication 78, p. 151-174, doi: 10.1144/GSL.SP.1994.078.01.13.

Hawkins, M.E., Dietzman, W.C., and Seward, J.M., 1963, Analyses of brines from oil-productive formations in south Arkansas and north Louisiana: U.S. Bureau of Mines, Report of Investigations 6282, 28 p.

Hubbert, M.K., 1953, Entrapment of petroleum under hydrodynamic conditions: American Association of Petroleum Geologists Bulletin, v. 37, p. 1954-2026.

Kesler, S.E., Appold, M.S., Martini, A.M., Walter, L.M., Huston, T.J., and Kyle, J.R., 1995, Na-Cl-Br systematics of mineralizing brines in Mississippi Valley–type deposits: Geology, v. 23, p. 641-644, doi: 10.1130/0091-7613(1995)023<0641:NCBSOM>2.3.CO;2.

Liégeois, J.P., Benhallou, A., Azzouni-Sekkal, A., Yahiaouni, R., and Bonin, B., 2005, The Hoggar swell and volcanism: Reactivation of the Precambrian Tuareg shield during Alpine convergence and West African Cenozoic volcanism, *in* Foulger, G.R., Natland, J.H., Presnall, D.C., and Anderson, D.L., eds., Plates, plumes and paradigms: Geological Society of America Special Paper 388, p. 379-400, doi: 10.1130/0-8137-2388-4.379.

McCaffrey, M.A., Lazar, B., and Holland, H.D., 1987, The evaporation path of seawater and coprecipitation of Br^- and K^+ with halite: Journal of Sedimentary Petrology, v. 57, p. 928-937, doi: 10.1306/212F8CAB-2B24-11D7-8648000102C1865D.

Moldovanyi, E.P., and Walter, L.M., 1992, Regional trends in water chemistry, Smackover Formation, southwest Arkansas: Geochemical and physical controls: American Association of Petroleum Geologists Bulletin, v. 76, p. 864-894.

Morad, S., Ben Ismail, H.N., De Ros, L.F., Al-Aasm, I.S., and Serrhini, N.-E., 1994, Diagenesis and formation water chemistry of Triassic reservoir sandstones from southern Tunisia: Sedimentology, v. 41, p. 1253-1272, doi: 10.1111/j.1365-3091.1994.tb01452.x.

Munz, I.A., 2001, Petroleum inclusions in sedimentary basins: systematics, analytical methods and applications: Lithos, v. 55, p. 195-212, doi: 10.1016/S0024-4937(00)00045-1.

Oakes, C.S., Bodnar, R.J., and Simonson, J.M., 1990, The system NaCl-$CaCl_2$-H_2O 1: The ice liquidus at 1 atm total pressure: Geochimica et Cosmochimica Acta, v. 54, p. 603-610, doi: 10.1016/0016-7037(90)90356-P.

Rittenhouse, G., 1967, Bromine in oil-field waters and its use in determining possibilities of origin of these waters: American Association of Petroleum Geologists Bulletin, v. 51, p. 2430-2440.

Roedder, E, 1984, Fluid inclusions: Mineralogical Society America, Reviews in Mineralogy, vol. 12, Washington, D.C., 644 p.

Sibson, R.H., 2000, Tectonic controls on maximum sustainable overpressure: Fluid redistribution from stress transitions: Journal of Geochemical Exploration, v. 69-70, p. 471-475, doi: 10.1016/S0375-6742(00)00090-X.

Smalley, P.C., and Muggeridge, A.H., 2010, Reservoir compartmentalization: get it before it gets you, *in* Jolley, S.J., Fisher, Q.J., Ainsworth, R.B., Vrolijk, P.J., and Delisle, S., eds., Reservoir Compartmentalization: Geological Society, London, Special Publication 347, p. 25-41, doi: 10.1144/SP347.3.

Stampfli, G.M., and Borel, G.D., 2002, A plate tectonic model for the Paleozoic and Mesozoic constrained by dynamic plate boundaries and restored synthetic oceanic isochrons: Earth and Planetary Science Letters, v. 196, p. 17-33, doi: 10.1016/S0012-821X(01)00588-X.

Turner, P., and Sherif, H., 2007, A giant late Triassic–Early Jurassic evaporitic basin on the Saharan Platform, North Africa, *in* Schreiber, B.C., Lugli, S., and Bąbel, M., eds., Evaporites through space and time: Geological Society, London, Special Publication 285, p. 87-105, doi: 10.1144/SP285.6.

Walderhaug, O., 1994, Precipitation rates for quartz cement in sandstones determined by fluid-inclusion microthermometry and temperature history modeling: Journal of Sedimentary Research, v. 64, p. 324–333.

Walter, L.M., Stueber, A.M., and Huston, T.J., 1990, Br-Cl-Na systematics in Illinois basin fluids: Constraints on fluid origin and evolution: Geology, v. 18, p. 315-318, doi: 10.1130/0091-7613(1990)018<0315:BCNSII>2.3.CO;2.

Wilson, M., and Guiraud, R., 1992, Magmatism and rifting in Western and Central Africa, from Late Jurassic to Recent times: Tectonophysics, v. 213, p. 203–225, doi: 10.1016/0040-1951(92)90259-9.

Wilson, M., Guiraud, R., Moreau, C., and Bellion, Y.J.C., 1998, Late Permian to Recent magmatic activity on the African-Arabian margin of Tethys, *in* MacGregor, D.S., Moody, R.T.J., and Clark-Lowes, D.D., eds., Petroleum geology of North Africa: Geological Society, London, Special Publication 132, p. 231-263, doi: 10.1144/GSL.SP.1998.132.01.14.

Yahi, N., Schaefer, R.G., and Littke, R., 2001, Petroleum generation and accumulation in the Berkine Basin, eastern Algeria: American Association of Petroleum Geologists Bulletin, v. 85, p. 1439-1467, doi: 10.1306/8626CAD7-173B-11D7-8645000102C1865D.

Zeroug, S., Bounoua, N., and Lounissi, R., 2007, Well Evaluation Conference (WEC) Algérie 2007, Sonatrach-Schlumberger: Wetmore Printing Company, Houston, 536 p.

List of Figures and Tables

Figure 1: Location of the study area in the Illizi Basin, Algeria. Extent of Triassic-Jurassic evaporitic basin and clastics adapted from Turner and Sherif (2007) and Galeazzi et al. (2010). Regions of present-day high pressured Triassic and Ordovician systems from Chiarelli (1978). Transect line corresponds to Figure 5.

Figure 2: 1D burial history model (Well G) for the study area in the Illizi Basin (modified from English et al., 2016c).

Figure 3: Salinity [A] and homogenization temperature [B] distributions from aqueous fluid inclusions in the Upper Ordovician sandstones from the study area in the Illizi Basin. Salinities are in wt.% NaCl equivalent.

Figure 4: Petrographic evidence indicating that the higher-salinity, lower temperature aqueous fluid inclusions post-date the lower-salinity, higher temperature aqueous fluid inclusions. A: Lower temperature, higher-salinity aqueous inclusions trapped in late-stage barite cements. B: Higher-salinity secondary inclusions observed in a microfracture that cuts across a detrital quartz grain and quartz overgrowth. C: Higher-salinity secondary inclusions observed in a microfracture that cuts across a quartz overgrowth containing lower salinity, higher temperature primary inclusions. Salinities are in wt.% NaCl equivalent.

Figure 5: Na-Cl-Br systematics for basinal brines (based on Kesler et al., 1995). Solid line shows the compositional change during progressive seawater evaporation (data from McCaffrey et al., 1987 and Carpenter, 1978). The Ordovician formation water in this study is characterized by relatively low Cl/Br and Na/Br ratios that are consistent with residual brines generated during progressive evaporation of seawater beyond the point of halite precipitation. The Triassic formation waters in the El Borma Field (Fig. 1, Morad et al., 1994) also have a similar signature. These systematics are not impacted by subsequent dilution with meteoric water, and exchange reactions involving Na and Ca would result in data plotting off of the defined seawater evaporation and halite dissolution trends (Kesler et al., 1995).

Figure 6: Schematic cross-section of the Illizi, Berkine and Oued Mya basins (modified from Galeazzi et al., 2010). Triassic deposits directly overlie Cambro-Ordovician strata along major Hercynian structures north of the study area. High-salinity brines may have originally infiltrated the Cambro-Ordovician sequence at these locations via density-driven brine reflux during or after the deposition of the Triassic evaporitic sequence. Aqueous fluid inclusions in

Ordovician sandstones record the migration of a high-salinity brine into the study area during cooling and exhumation of the Illizi Basin. Lateral flow within the Cambro-Ordovician sequence is interpreted to be focused between the underlying crystalline basement and the overlying Lower Silurian shales. Present day, the sub-salt area around Hassi Messaoud and Hassi R'Mel is characterized by an overpressured system while an active gravity-driven hydrodynamic flow system has been interpreted at multiple stratigraphic levels on the southern margin of the exhumed Illizi Basin (Chiarelli, 1978). The burial history of the study area in the Illizi Basin is shown in Figure 2 and illustrates the major exhumation of the Illizi Basin during the Cenozoic. Section line is shown on Figure 1.

Figure 7: Formation water salinity-depth trends from (1) Jurassic to Cretaceous strata in southern Arkansas and northern Louisiana (Dickey, 1969; data from Hawkins et al., 1963), and (2) the northern North Sea (Gran et al., 1992; including data from Egeberg and Aagaard, 1989). The higher salinity formation waters in the Gulf Coast example are interpreted to be derived from an underlying evaporitic unit (Moldovanyi and Walter, 1992; Hanor, 1994), whereas no underlying evaporites are known to occur in the northern North Sea example (Gran et al., 1992; Bjørlykke and Gran, 1994). The high temperature, low-salinity fluid inclusions in the Illizi Basin study area lie along the northern North Sea trend, whereas the low temperature, high-salinity fluid inclusions plot along the southern Arkansas-northern Louisiana trend. This dramatic change in the salinity-depth relationship recorded by the fluid inclusion dataset indicates that a significant lateral transport of brine likely occurred within the basin at some point during its history.

Table 1: Compositional analysis of formation water in the Ordovician sandstone of the Illizi Basin

Table 2: Summary of fluid inclusion data from Upper Ordovician sandstone in the Illizi Basin

Figure 1

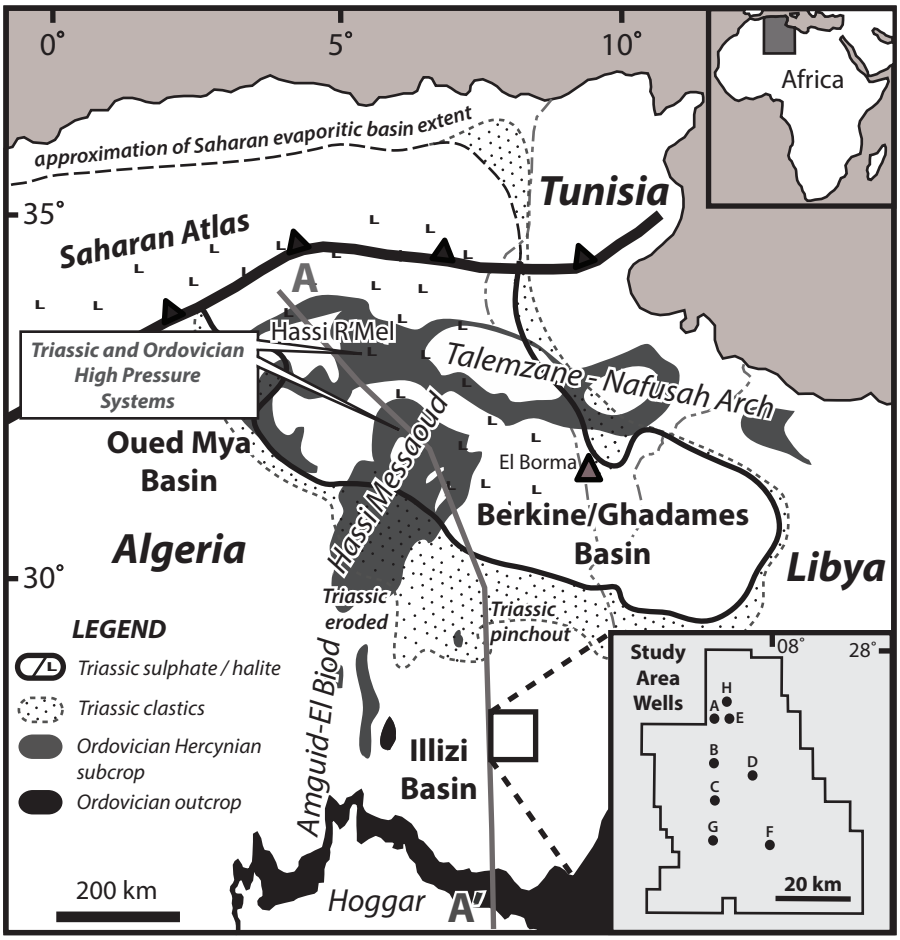
0°
5°
10°
Africa
approximation of Saharan evaporitic basin extent
Tunisia
35°
Saharan Atlas
A
Hassi R'Mel
Triassic and Ordovician High Pressure Systems
Talemzane - Nafusah Arch
Oued Mya Basin
Hassi Messaoud
El Borma
Berkine/Ghadames Basin
Algeria
Libya
30°
Triassic eroded
Triassic pinchout
LEGEND
Triassic sulphate / halite
Triassic clastics
Ordovician Hercynian subcrop
Ordovician outcrop
Amguid-El Biod
Illizi Basin
200 km
Hoggar
A'
Study Area Wells
08°
28°
H
A
E
B
D
C
G
F
20 km

Figure 2

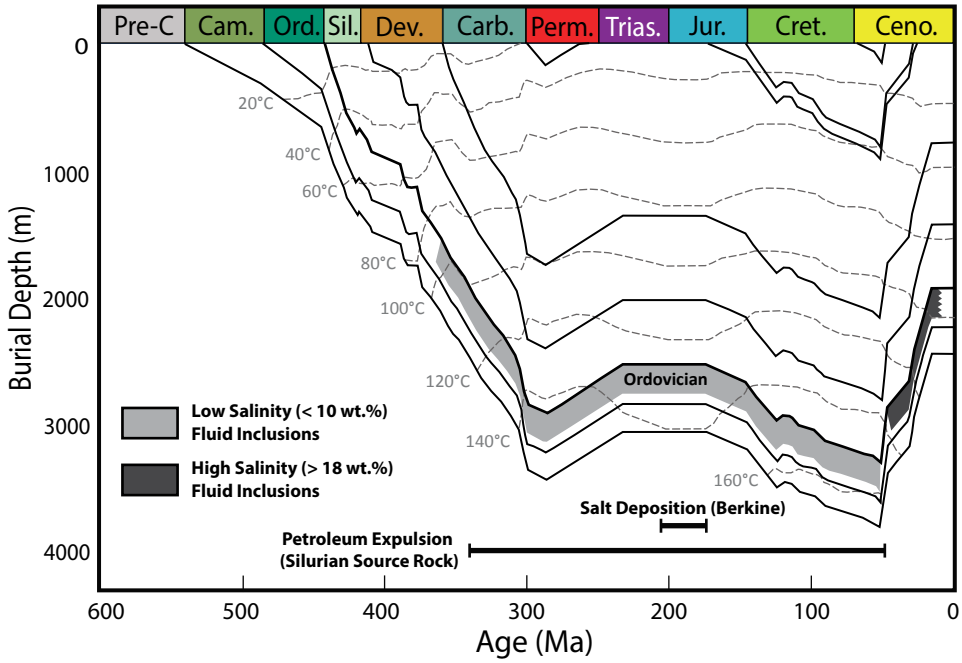
Pre-C
Cam.
Ord.
Sil.
Dev.
Carb.
Perm.
Trias.
Jur.
Cret.
Ceno.
0
1000
2000
3000
4000
Burial Depth (m)
20°C
40°C
60°C
80°C
100°C
120°C
140°C
160°C
Ordovician
Low Salinity (< 10 wt.%)
Fluid Inclusions
High Salinity (> 18 wt.%)
Fluid Inclusions
Salt Deposition (Berkine)
Petroleum Expulsion
(Silurian Source Rock)
600
500
400
300
200
100
0
Age (Ma)

Figure 3

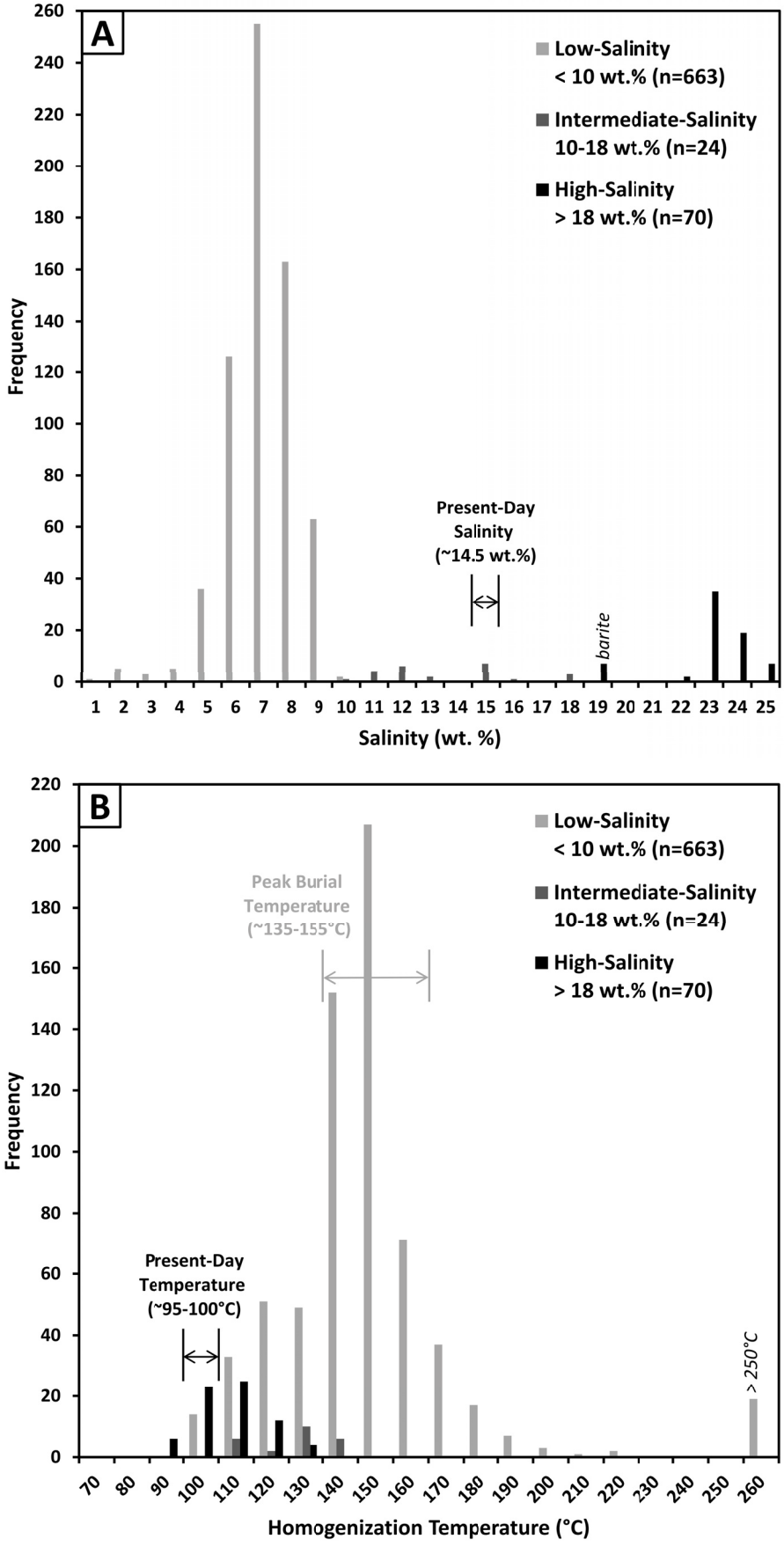
A
Low-Salinity
< 10 wt.% (n=663)
Intermediate-Salinity
10-18 wt.% (n=24)
High-Salinity
> 18 wt.% (n=70)
Present-Day
Salinity
(~14.5 wt.%)
barite
Frequency
Salinity (wt. %)
B
Low-Salinity
< 10 wt.% (n=663)
Intermediate-Salinity
10-18 wt.% (n=24)
High-Salinity
> 18 wt.% (n=70)
Peak Burial
Temperature
(~135-155°C)
Present-Day
Temperature
(~95-100°C)
> 250°C
Frequency
Homogenization Temperature (°C)

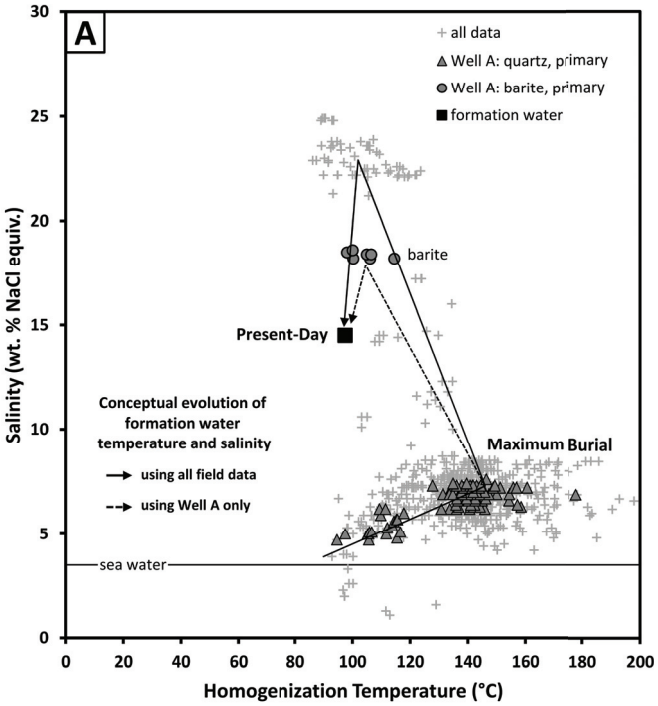

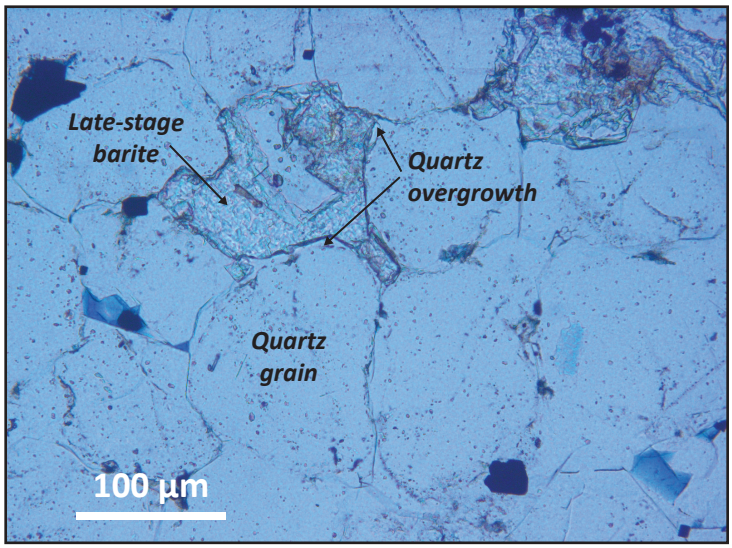

Well A: 1916.6 m

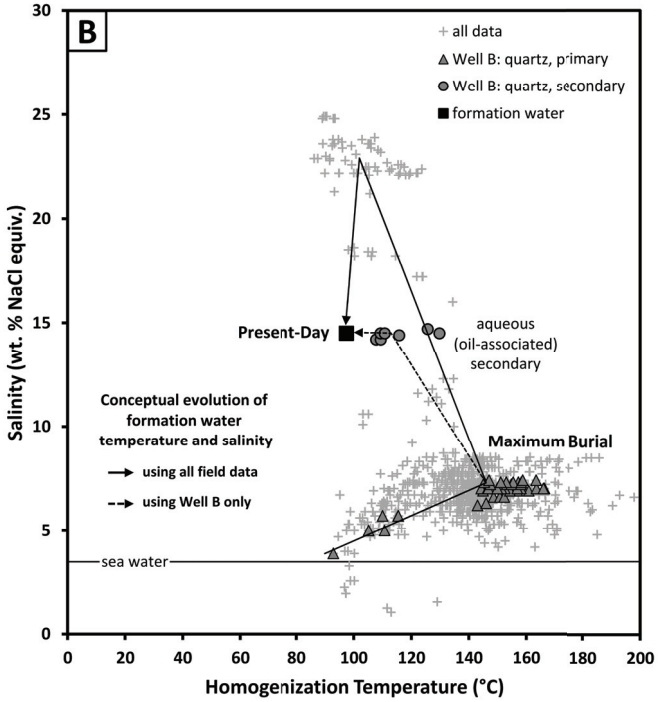

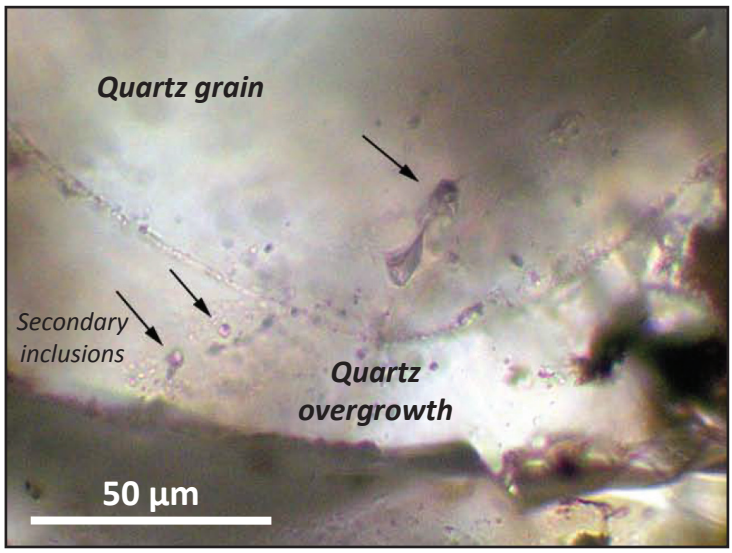

Well B: 1914.5 m

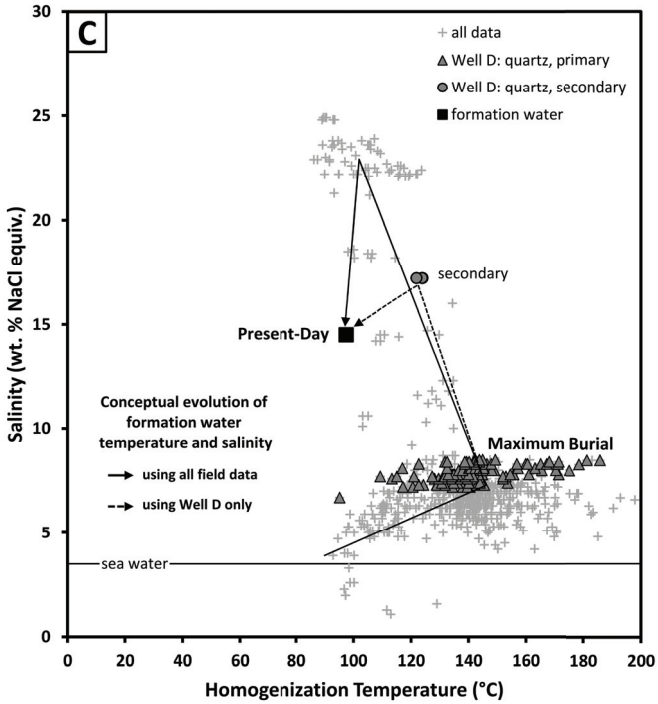

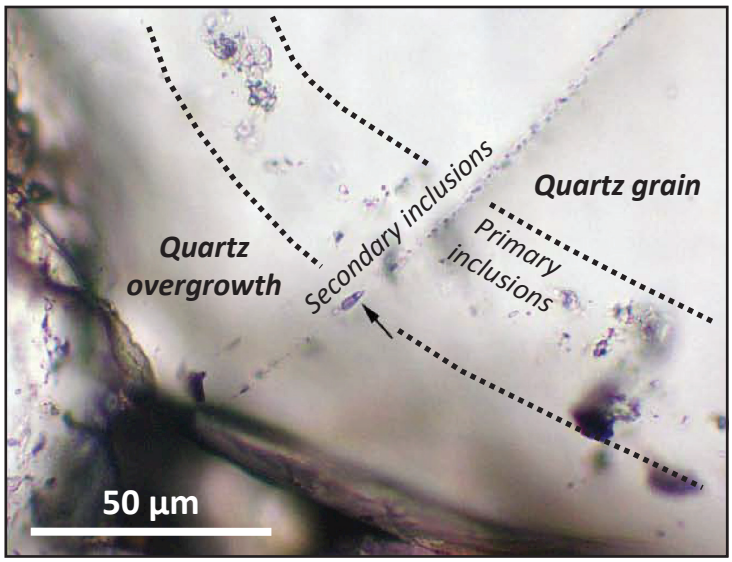

Well D: 1917.1 m

Figure 5

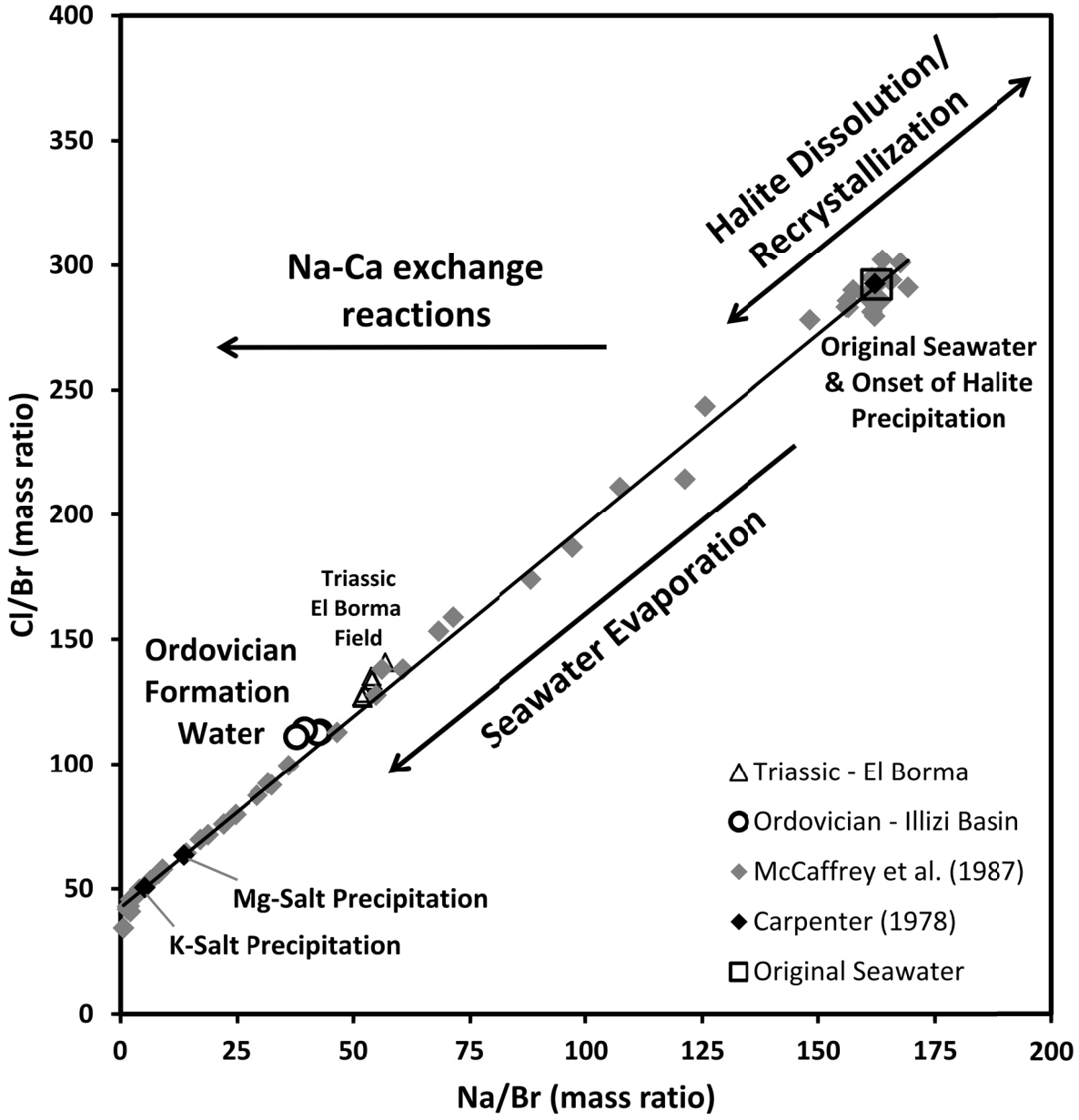
Halite Dissolution/
Recrystallization
Na-Ca exchange
reactions
Original Seawater
& Onset of Halite
Precipitation
Triassic
El Borma
Field
Ordovician
Formation
Water
Seawater Evaporation
Mg-Salt Precipitation
K-Salt Precipitation
Triassic - El Borma
Ordovician - Illizi Basin
McCaffrey et al. (1987)
Carpenter (1978)
Original Seawater
Cl/Br (mass ratio)
Na/Br (mass ratio)
0
50
100
150
200
250
300
350
400
0
25
50
75
100
125
150
175
200

Figure 6

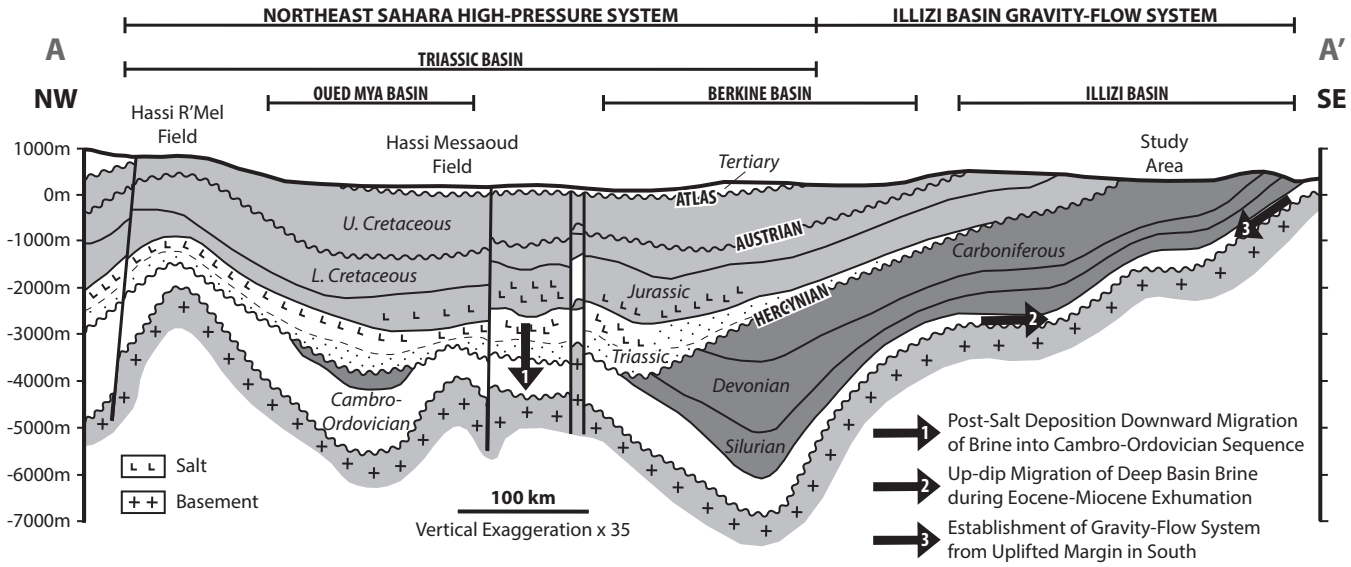
NORTHEAST SAHARA HIGH-PRESSURE SYSTEM
ILLIZI BASIN GRAVITY-FLOW SYSTEM
A
A'
TRIASSIC BASIN
NW
SE
OUED MYA BASIN
BERKINE BASIN
ILLIZI BASIN
Hassi R'Mel Field
Hassi Messaoud Field
Study Area
1000m
0m
-1000m
-2000m
-3000m
-4000m
-5000m
-6000m
-7000m
Tertiary
ATLAS
AUSTRIAN
HERCYNIAN
U. Cretaceous
L. Cretaceous
Jurassic
Triassic
Carboniferous
Devonian
Silurian
Cambro-Ordovician
Salt
Basement
100 km
Vertical Exaggeration x 35
1
2
3
Post-Salt Deposition Downward Migration of Brine into Cambro-Ordovician Sequence
Up-dip Migration of Deep Basin Brine during Eocene-Miocene Exhumation
Establishment of Gravity-Flow System from Uplifted Margin in South

Figure 7

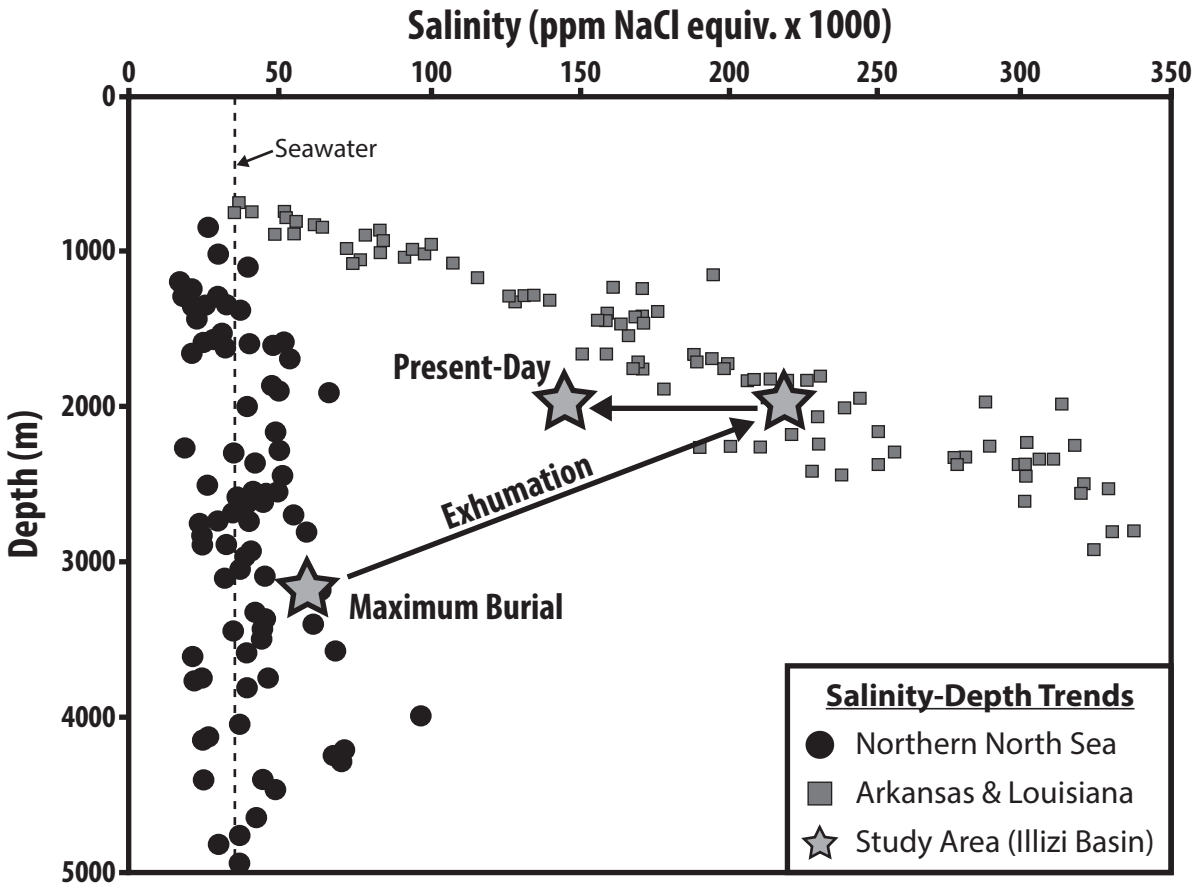
Salinity (ppm NaCl equiv. x 1000)
0
50
100
150
200
250
300
350
Depth (m)
0
1000
2000
3000
4000
5000
Seawater
Present-Day
Exhumation
Maximum Burial
Salinity-Depth Trends
Northern North Sea
Arkansas & Louisiana
Study Area (Illizi Basin)

TABLE 1: Compositional analysis of formation water in the Ordovician sandstone of the Illizi Basin

By Volume (mg/L)

Field / Well Reference	Well H (pre-frac)	
Sample Reference	1.11	1.15
Physicochemical Parameters		
pH @ 19.9 °C (pH units)	3.95	4.18
Resistivity @ 20 °C (ohm.m)●	0.0650	0.0643
Density @ 20.03 °C (kg/L)*	1.1098	1.1115
Anionic Species (mg/L)		
Chloride	96,398	97,835
Sulphate	3	2
Bromide	846	881
Nitrate	3.0	2.6
Phosphate	-	-
Iodide	< 3	< 3
Bicarbonate	< 11	< 11
Carbonate	0	0
Hydroxide	0	0
Formate	28.2	20.7
Acetate	155	156
Propionate	12	12
Butyrate	2.6	2.3
iso -Valerate	< 2	< 2
Cl:Br	*114*	*111*
	HCl Preserved	
Sample Reference	1.13	1.17
Density @ 20.06 °C (kg/L)*	1.1104	1.1121
Boron *(as Tetraborate $B_4O_7^{2-}$)*	22	23
Cationic Species (mg/L)		
Lithium	52	55
Barium	523	677
Strontium	695	731
Calcium	20,449	21,395
Magnesium	1,880	1,953
Sodium	33,496	33,352
Potassium	2,203	2,082
Iron	520	458
Copper	< 1	< 1
Zinc	< 2	< 2
Manganese	41	44
Aluminium	< 2	< 2
Ammonium	87.9	88.7
Tetra Methyl Ammonium	< 22	< 22
Total Species (mg/L)		
Total Barium	529	678
Total Iron	508	485
Elements (mg/L)		
Phosphorus	< 6	< 6
Silicon	13	15
Sulphur	23	19
Total Cl^- equivalent (mg/L)	96,910	98,356
Total Na^+ equivalent (mg/L)	63,095	64,134
Total NaCl equivalent (mg/L)	160,004	162,490
TDS (calculated) (mg/L)	158,467	160,947
Cation/Anion Balance	100.40%	100.55%
Cation/Anion Bias	0.40%	0.55%

By Volume (mg/L)

Field / Well Reference	Well D (post-frac)	
Sample Reference	2-26	2-27
Physiochemical Parameters		
pH @ 19.4 ± 1.6 °C (pH units)	5.87	5.65
Resistivity @ 20 °C (ohm.m)●	0.0678	0.0671
Density @ 20.07 ± 0.11 °C (kg/L)*	1.1108	1.1126
Anionic Species (mg/L)		
Chloride	95,358	96,926
Sulphate	< 1	< 1
Bromide	843	861
Nitrate	2.4	2.9
Phosphate	< 2	< 1
Iodide	3.9	4.0
Bicarbonate	39	33
Carbonate	0	0
Hydroxide	0	0
Formate	3.7	3.2
Acetate	86	87
Propionate	4.2	4.3
Butyrate	< 1	< 1
iso -Valerate	< 1	< 1
Cl:Br	*113*	*113*
Boron	20	20
Cationic Species (mg/L)		
Lithium	75	77
Barium	2,994	3,122
Strontium	1,404	1,449
Calcium	18,337	18,436
Magnesium	1,494	1,519
Sodium	36,183	36,556
Potassium	1,025	1,044
Iron	73	78
Copper	< 2	< 2
Zinc	< 1	< 1
Manganese	10.1	10.2
Aluminium	< 11	< 11
Ammonium	115	121
Tetra Methyl Ammonium	197	182
Total Species (mg/L)		
Total Barium	2,959	3,059
Total Iron	158	161
Elements (mg/L)		
Phosphorus	< 11	< 11
Silicon	18	19
Sulphur	< 21	< 21
Total Cl^- equivalent (mg/L)	95,847	97,420
Total Na^+ equivalent (mg/L)	62,914	63,534
Total NaCl equivalent (mg/L)	158,760	160,954
TDS (calculated) (mg/L)	157,974	160,250
Cation/Anion Balance	101.22%	100.57%
Cation/Anion Bias	1.22%	0.57%

TABLE 2: Summary of Fluid Inclusion Data from Upper Ordovician Sandstone in the Illizi Basin

Category	n	Ave. T_h(°C)	±	T_{ice} (°C)	±	Salinity (wt.%)†	±
Low Salinity (<10 wt.%)	663	142.6	25.6	-3.9	1.7	6.6	1.2
Intermediate Salinity (10-18 wt.%)	24	121.6	10.4	-9.2	2.2	13.1	2.3
High Salinity (>18 wt.%)	70	102.9	10.0	-20.1	2.2	22.5	1.6

† *Salinities are in wt.% NaCl equivalent*